

Dynamic link budget simulation

*Original*

Dynamic link budget simulation / Mcmanamon, P.; Visintin, Monica. - ELETTRONICO. - (2013), pp. 1-8. ( TTC 2013, 6th ESA International Workshop on Tracking, Telemetry and Command Systems for Space Applications Darmstadt Germany 10-13 Sept. 2013).

*Availability:*

This version is available at: 11583/2514292 since:

*Publisher:*

ESA

*Published*

DOI:

*Terms of use:*

This article is made available under terms and conditions as specified in the corresponding bibliographic description in the repository

*Publisher copyright*

(Article begins on next page)

## DYNAMIC LINK BUDGET SIMULATION

Paul McManamon<sup>1</sup>, Monica Visintin<sup>2</sup>

<sup>1</sup> ESA/ESTEC, Keplerlaan 1, Noordwijk, The Netherlands, [Paul.McManamon@esa.int](mailto:Paul.McManamon@esa.int).

<sup>2</sup> Dipartimento di Elettronica e Telecomunicazioni, Politecnico di Torino, Corso Duca degli Abruzzi 24, Torino, Italy, [monica.visintin@polito.it](mailto:monica.visintin@polito.it)

### I. INTRODUCTION

A new simulator named DLBS (Dynamic Link Budget Simulator) was written to simulate the time-varying communication link between a vehicle that re-enters the atmosphere from the outer space, and a ground station. During the vehicle descent trajectory, communications blackouts typically occur due to the effects of plasma that forms around the vehicle.

A companion simulator, AIPT (Antenna In Plasma Tool)[1,7], evaluates the electric field at the input of the receiving ground station antenna, taking into consideration the vehicle and its transmitting antenna structures and the characteristics of plasma; the vectors are evaluated every 10 s during the vehicle descent phase and stored in a file. DLBS processes the data read from the AIPT output file and evaluates the corresponding channel transfer functions. DLBS then allows to simulate the typical telemetry and tele-command links, using both CCSDS standardized [2,3] and some non standard channel encoding schemes and modulations. For each generated frame, DLBS uses a channel transfer function obtained by adequately interpolating the two nearest transfer functions evaluated from the AIPT output data. DLBS includes realistic frame, frequency, phase and symbol synchronization, so that synchronization errors are also included as source of performance degradation, and measures the bit (BER) and frame (FER) error rates, both as an average and at frame level so that it is possible to appreciate the dynamic system behavior.

The paper is organized as follows: Sect. II gives the formulas used to generate the time-varying channel transfer function from the electric field vector and discusses other parameters of the channel model; Sect. III describes the considered simulation scenario; Sect. IV gives a brief overview of the DLB simulator ; Sect. V provides some simulation results and Sect VI draws the conclusions.

### II. FROM THE ELECTRIC FIELD VECTORS TO THE CHANNEL MODEL

#### A. The channel transfer function

The companion software AIPT [1] simulates the transmission of a single carrier at frequency  $f_0$  and power  $P_T$  from the re-entry vehicle onboard antenna and evaluates the electric field vector present at the input of the receiving antenna. Due to the required CPU times, only some frequencies  $f_0$  can be analyzed in practice. AIPT simulations were run using  $f_0 = f_c + m\Delta_f$  with  $f_c$  center frequency (either 2.26 GHz or 7.19 GHz),  $m=0,\pm 1,\pm 2$  and  $\Delta_f=200$  kHz. The square modulus of the channel transfer function  $H(f)$  from TX to RX antenna (included) can be evaluated at each analyzed frequency as [4]

$$|H(f_0)|^2 = \frac{D}{P_T} \frac{G_R \lambda^2}{4\pi} pq \quad (1)$$

where:

- $D$  is the power flux density ( $\text{W}/\text{m}^2$ ) at the receiving antenna, which can be evaluated from the electric field vector  $\mathbf{E} = E_\theta \hat{\theta} + E_\phi \hat{\phi} = (E_{\theta,r} + jE_{\theta,i})\hat{\theta} + (E_{\phi,r} + jE_{\phi,i})\hat{\phi}$  generated by AIPT as

$$D = \frac{E_{\theta,r}^2 + E_{\theta,i}^2 + E_{\phi,r}^2 + E_{\phi,i}^2}{2\eta_0}, \quad \eta_0 \approx 120\pi \quad (2)$$

- $G_R$  is the RX antenna gain
- $\lambda=1/f_0$  is the wavelength
- $p$  is the polarization mismatch loss

$$p = \frac{|\mathbf{E} \cdot \mathbf{h}|^2}{|\mathbf{E}|^2 |\mathbf{h}|^2} = \frac{|\mathbf{E} \cdot \hat{\mathbf{h}}|^2}{|\mathbf{E}|^2}, \quad (3)$$

being  $\hat{\mathbf{h}}$  the normalized effective length of the RX antenna, with  $\hat{\mathbf{h}} = (\hat{\theta} + j\hat{\phi})/\sqrt{2}$  for an LHCP (Left Hand Circular Polarized) antenna and  $\hat{\mathbf{h}} = (\hat{\theta} - j\hat{\phi})/\sqrt{2}$  for an RHCP (Right Hand Circular Polarized) antenna, and  $\cdot$  the dot (scalar) product of the two vectors

- $q$  is the impedance mismatch factor, which can be written as

$$q = 1 - \frac{|\text{VSWR} - 1|^2}{|\text{VSWR} + 1|^2} \quad (4)$$

in terms of the voltage standing wave ratio (VSWR) of the transmission line.

The phase of the transfer function  $H(f_0)$  is the phase of the complex number  $\mathbf{E} \cdot \hat{\mathbf{h}}$  plus the phase of the RX antenna load impedance  $Z_L$  at frequency  $f_0$ . We assumed that the phase  $Z_L$  does not change in the frequency band of the transmitted signal (i.e. it does not depend on  $f_0$ ) so that the phase of  $H(f_0)$  can be considered equal to the phase of  $\mathbf{E} \cdot \hat{\mathbf{h}}$  (the phase shift due to  $Z_L$  is recovered by the carrier phase synchronizer of the receiver).

In the software, it was assumed that  $q=1$ , and that both polarizations (LHCP and RHCP) are available at the receiver (at least in this phase of analysis), so that two transfer functions are evaluated for each data set produced by AIPT: we will refer to them as LHCP and RHCP channels. It is furthermore assumed that the ground station antenna has a high gain  $G_R$  and it is perfectly pointed towards the vehicle; it is possible to include a static pointing loss by decreasing the ground station gain.

Actually the electric field vectors are generated by AIPT not only at the exact assumed position of the RX antenna, but at 25 directions  $(\theta, \varphi)$  in a cone of aperture 4 degrees around the nominal direction of the RX antenna; the rationale behind this choice is that the asset of the vehicle is not exactly known, and therefore the direction of the main lobe of the TX antenna radiation pattern might not be the nominal one. Note that the electric field vectors provided by AIPT include the pointing loss (which depends on  $(\theta, \varphi)$ ) and the on-board antenna gain, while the ground station gain and polarization are added by DLBS. The channel transfer function  $H(f_0)$  is considered valid for both the uplink (tele-command) and downlink (telemetry); on the contrary bit rates, modulation, coding, and transmitted powers are different in the two links.

The RF signals are simulated through their complex envelopes, and therefore the channel transfer function  $H(f)$  must be shifted to baseband to get the correct results.

The channel is simulated using block processing [5]: given a portion of  $M$  samples of the signal  $x(n\delta_t)$  at the output of the transmitter, zero padding is used to get a vector  $\mathbf{x}$  with  $N=2M$  samples, then the signal  $y(n\delta_t)$  at the output of the channel is found as the IFFT (Inverse Fast Fourier Transform) of  $Y(k)=X(k)C(k\delta_f)$ , where  $X(k)$  is the  $k$ -th value of the FFT of  $\mathbf{x}$  and  $C(k\delta_f)$  are samples of  $H(f-f_c)$ , being  $\delta_f=1/(N\delta_t)$ . The method "overlap and add" [5] is used to generate  $M$  output samples for each  $M$  input samples. The values  $C(k\delta_f)$  are evaluated through interpolation/extrapolation from the AIPT output values  $H(f_c + m\Delta_f)$ ,  $m=0, \pm 1, \pm 2$ ,  $\Delta_f=200$  kHz. Note that the frequency spacing  $\Delta_f=200$  kHz was chosen in order to minimize the costs of running AIPT, while keeping a reasonable number of values  $H(f_c + m\Delta_f)$ , assuming a maximum telemetry information bit rate around 200 kbit/s. On the other side, the frequency interval  $\delta_f=1/(N\delta_t)$  depends on the simulation sampling interval  $\delta_t=T_b/N_b$ , where: a)  $T_b=1/R_b$  is the channel bit interval, which depends on the information bit rate, the channel coding rate and the length of the frame preamble/synch marker, arbitrarily chosen by the user, b)  $N_b$  is the number of simulated samples per bit, set equal to 8 in DLBS. In general, then, there is no integer relationship between  $\delta_f$  and  $\Delta_f$ , and interpolation is required. DLBS accomplishes this task as follows:

- a) The channel impulse response at times  $n\delta_t$  is evaluated as

$$c(n\delta_t) \approx \sum_{m=-2}^2 H(f_c + m\Delta_f) e^{j2\pi m\Delta_f n\delta_t} \Delta_f \quad n = 0, K, N_h - 1 \quad (5)$$

(note that  $1/(\delta_t \Delta_f)$  is not an integer number, in general);

- b) zero padding with  $N-N_h$  zeros is performed, obtaining a vector  $\mathbf{c}$  with  $N$  values, and
- c) vector  $\mathbf{C}$  is obtained as FFT of vector  $\mathbf{c}$ . Element  $\mathbf{C}(k)$  is the required value  $C(k\delta_f)$ .

If the simulation sampling frequency  $1/\delta_t$  is much less than  $\Delta_f$ , then interpolation is not performed and  $\mathbf{C}(k)$  is set equal to  $H(f_c)$ .

In many cases, when the vehicle speed is large and plasma effects are relevant, the transfer function changes dramatically with the direction  $(\theta, \varphi)$ ; it is then more correct to refer to the transfer function as  $C(k\delta_f, \theta, \varphi)$ . Averaging the transfer function over the 4 degree cone considered by AIPT seems a reasonable choice for the prediction of the telecommunication system average performance. DLBS allows for averaging in terms of modulus and phase or in terms of real and imaginary parts of  $C(k\delta_f, \theta, \varphi)$ . The worst case transfer functions inside the cone is also of interest, and DLBS finds  $C(k\delta_f, \theta_w, \varphi_w)$  with  $(\theta_w, \varphi_w)$  such that

$$\sum_{m=-2}^2 |H(f_c + m\Delta_f, \theta_w, \varphi_w)|^2 = \min_{\theta, \varphi} \sum_{m=-2}^2 |H(f_c + m\Delta_f, \theta, \varphi)|^2 \quad (6)$$

(minimum energy of the impulse response) so that the user can also simulate the worst-case system.

The vehicle, during its descent, changes its speed thus modifying the plasma conditions and the channel transfer function. AIPT evaluates the electric field vector at the receiver every  $\Delta_t=10$  s (again to limit the AIPT simulation costs), and therefore several transfer functions  $C(k\delta_f, i\Delta_t)$  are available, which must be interpolated in the time domain. Due to the choice of simulating the channel in the frequency domain, the transfer function can be updated only every  $M\delta_t$  seconds, so that the  $m$ -th block of signal samples is filtered with the  $m$ -th transfer function  $C(k\delta_f, mM\delta_t)$ . If, for simplicity,  $\Delta_t < mM\delta_t < 2\Delta_t$ , then  $C(k\delta_f, mM\delta_t)$  is obtained from  $C(k\delta_f, \Delta_t)$  and  $C(k\delta_f, 2\Delta_t)$  as:

$$C(k\delta_f, mM\delta_t) = C(k\delta_f, \Delta_t)(2 - mM\delta_t / \Delta_t) + C(k\delta_f, 2\Delta_t)(mM\delta_t / \Delta_t - 1) \quad (7)$$

The above equation performs linear time-interpolation in terms of real and imaginary parts of  $C(k\delta_f, i\Delta_t)$ , but DLBS allows for interpolation also in terms of modulus and phase. The user can also ask DLBS to find the worst-case transfer function for the entire vehicle trajectory and check the performance of the transmission system for this static case.

### B. Presence or absence of fast fading

Basically, plasma generates a channel transfer function with “holes” at some frequencies (see Fig. 5), as it happens in the transmission between a base station and a moving phone in wireless terrestrial communications. In this last case, several paths link the transmitter to the receiver, and, depending on the specific frequency and position of the mobile, constructive or destructive interference occurs. When the phone moves, the received power changes at a rate which depends on the mobile speed  $v$ , giving rise to the fast fading phenomenon. In the typical mathematical model of fast fading, the transmitted signal complex envelope is multiplied by a complex random process  $g(t)=\rho(t)e^{j\psi(t)}$  with phase  $\psi(t)$  uniformly distributed in  $[-\pi, \pi]$  and modulus  $\rho(t)$  with Rayleigh probability density function and autocorrelation function proportional to the zero-th order Bessel function  $J_0(2\pi f_c \tau v/c)$  ( $c$  identifies the light speed). Therefore, the question arises about the fact that fast fading also occurs in the case of a re-entry vehicle surrounded by plasma. In both cases one of the two antennas of the link is moving and multipath effects are visible, but in the case of a re-entry vehicle, the origin of multipath (plasma) moves together with the vehicle, while in the case of terrestrial mobile communications, multipath is generated by reflecting or diffracting objects (like buildings) that do not move. In the case of terrestrial mobile communications, the strength of the electric field depends on the position of the mobile and fading occurs if and only if the mobile changes its position in time (speed  $v$  different from zero). In the case of re-entry vehicle, on the contrary, multipath does not change with the position of the vehicle along its trajectory, as far as short time intervals are considered (so short that the plasma parameters are not significantly changed), the received power changes only for the changed distance between transmitter and receiver and slowly changing plasma characteristics. Therefore, fast fading should not be included in the channel model for the case of a re-entry vehicle.

### C. Doppler frequency shift

The vehicle speed is very high (in the evaluation of the descent trajectories the maximum Mach number 27 was reached, corresponding to 9.2 km/s), and a non-negligible Doppler frequency shift is present in the received signal. However, the vehicle trajectory can be predicted with relatively high precision so that a speed prediction error of only  $\Delta_v=10$  m/s is expected [6]. It is therefore possible to dynamically pre-compensate most of the Doppler frequency shift, but a frequency shift  $D_f = \Delta v f_c / c$  must be included in the model of the received signal; in particular,  $D_f=75.3$  Hz for  $f_c=2.26$  GHz (S band) and  $D_f=240$  Hz for  $f_c=7.19$  GHz (X band). The effects of this residual Doppler frequency shift much depend on the signal bit rate. For example, assuming a Differential Quaternary Phase Shift Keying (DQPSK) modulation in the S-band, the phase error in a symbol interval is  $2\pi D_f 2T_b$  and it ranges from 0.0022 rad for the case of telemetry with information bit rate 200 kbit/s and channel coding rate 1/2, to 0.12 rad (6.8 deg) for the case of uncoded telecommand with information bit rate equal to 8 kbit/s. In the case of telemetry, a second order carrier phase synchronizer with closed loop is in general sufficient to compensate this residual Doppler frequency shift, provided that the loop noise equivalent bandwidth is larger than  $D_f$ ; otherwise a frequency synchronizer is required, which for example can exploit the synch marker to estimate  $D_f$  and remove its effects on the corresponding frame. In the case of telecommand, a direct sequence spread spectrum technique can be used to reduce the effects of the residual Doppler frequency shift.

As the vehicle moves, also the propagation delay changes, and therefore the symbol synchronizer continuously has to adapt. However, also the changes in the propagation delay can be pre-computed and used to aid symbol synchronization; the symbol synchronizer must then essentially compensate the group delay variations due to plasma.

### III. CONSIDERED SCENARIO

Two types of re-entry vehicles were considered in AIPT [1,7]: a lift-guided capsule (ARD-like, Atmospheric Re-entry vehicle Demonstrator) and a lifting body (IXV-like, Intermediate eXperimental Vehicle). In the first case, the assumed information bit rate for telemetry is 100 kbit/s, while in the second case the bit rate is increased to 192 kbit/s, allowing for a couple of voice channels and some more control data. Tele-command bit rates are assumed equal to 8 kbit/s for the ARD-like vehicle and 72 kbit/s for the IXV-like vehicle, again assuming a couple of voice channels.

The assumed vehicle antenna gain is an 8.5 dBi LHC polarized aperture-coupled patch antenna, operating in the S band (2.26GHz), installed at different positions aboard the reentry vehicle. AIPT includes an electromagnetic model of the vehicle structure, and the evaluated electric field vectors at the ground station actually depend on the interaction between antenna and its position on the vehicle structure and plasma.

It is assumed that no complexity restrictions apply to the receiver in the IXV-like vehicle, so that it is possible to imagine that channel decoding can be performed onboard, while the ARD-like receiver is standard, with limited complexity. The vehicle can, in principle, use two transmitters (with a space-time encoder), but DLBS does not allow to simulate this case yet. The vehicle receiver noise figure is set equal to 4 dB (corresponding to a noise equivalent temperature 438.5 K), and the antenna gain is 8.5 dBi, so that the quality figure of the vehicle receiver is -17.9 dB/K.

Some analysis was carried out for the case in which the vehicle link is towards one of the TDRSS (Tracking and Data Relay Satellite System) satellites, but the large path loss and the constraints on the characteristics of the signal transmitted and received by the satellite prevent reliable communications. This paper focuses on the case of ground stations on ships at locations chosen to guarantee the link [6,7] during the entire vehicle descent trajectory. The ground station quality figure  $G_R/T$  is considered equal to 13.5 dB/K, while the antenna gain is 35 dBi. No restriction exists on the complexity of the ground station receiver; in particular, the case in which the ground station receives on both polarizations (RHC and LHC) and combines the two signals will be analyzed in Sect. V.

### IV. DLBS STRUCTURE

The simulator was specifically written to evaluate the time-varying channel transfer function for the case of re-entry vehicles, but, of course, it includes the main blocks of typical telemetry and tele-command links. In particular, DLBS allows to simulate most of the classical modulators (PSK, OQPSK, DPSK, FSK, GMSK), filters, some CCSDS (Consultative Committee for Space Data Systems) standard channel encoders and decoders (convolutional with rate  $\frac{1}{2}$ , Reed Solomon, turbo with rate  $\frac{1}{2}$  and  $\frac{1}{3}$ ), symbol and phase synchronizers, etc. Other system blocks (other encoders, mo-demodulators, etc.) can be easily added. DLBS is set so that one block corresponds to one frame, made of the encoded bits and the synchronization marker. Even if DLBS was specifically written for the case of a plasma channel, it can be also used for simulating the physical and link layers for typical satellite communication links in the absence of plasma.

The software was written using Python, a cross-platform interactive and object oriented programming language [8], which allows for easy vector and matrix manipulations through its added packages Numpy and Scipy; other packages are available for plots (Matplotlib) and graphic interfaces (WxPython). The execution times of Python programs are larger than the corresponding pure C programs, but the order of magnitude is similar; the DLBS turbo encoders and decoders are actually C functions embedded in Python.

### V. TELEMETRY CASE STUDY

Results will be described in this section for the IXV case transmitting telemetry at  $R_b=1/T_b=192$  kbit/s, with a turbo encoder (rate  $\frac{1}{2}$  frame length 1784 information bits) and corresponding synchronization marker (72 bits, as per CCSDS specifications), so that the resulting channel bit rate is  $R_c=1/T_c= 384.9$  kbit/s. We consider a 4PSK (Quaternary Phase Shift Keying, symbol rate 192.5 kbaud) modulator with a square-root-raised-cosine filter with roll-off 0.5, and a nonlinear amplifier with AM/AM and AM/PM characteristics shown in Fig. 1. One simulation block corresponds to one frame, i.e. 3648 channel bits, corresponding to 29184 complex samples. It is assumed that no residual Doppler frequency shift is present; and S-band transmission (carrier frequency 2.26 GHz) occurs from the antenna installed at side -Y of the vehicle.

The receiving antenna detects both RHC and LHC polarizations and two parallel receivers are present, followed by a maximal ratio combiner. Each receiver is made of a bandpass filter (bandwidth 384.9 kHz), an AGC, an ideal RF to baseband converter which outputs the complex envelope of the input signal, a matched filter; since channel bit error rate is an interesting parameter to monitor, the receiver includes also two zero-threshold detectors apart from the turbo decoder. The normalized loop noise equivalent bandwidths of the phase and symbol synchronizers are set equal to  $BLT_c = 5 \cdot 10^{-4}$  (bandwidth 192.4 Hz), the blind decision directed equalizer is an FIR filter with 32 taps and updating coefficient 0.001 with complex weights, initialized with a 1 in the 16<sup>th</sup> position. Perfect compensation of the Doppler frequency shift is assumed, and the frequency synchronizer is not simulated.

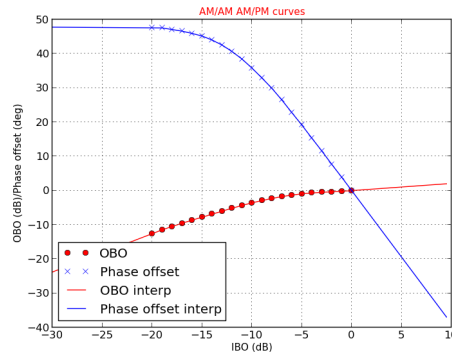


Fig. 1. AM/AM and AM/PM characteristics of the nonlinear amplifier

#### A. Static simulation

As a first case, a static channel simulation was considered with no time interpolation, and no averaging over the cone of 4 degree aperture; the worst case transfer function was chosen, corresponding to the case of Mach number 27 (9.2 km/s). DLBS was initially run in the absence of plasma (so that the channel just introduces attenuation) in order to get the reference case; then DLBS was run again with plasma on the same link. The transmitted power was varied so as to measure channel or information bit error rates approximately in the range  $[10^{-4}, 0.5]$ . The values of transmitted power are actually unrealistic (always less than 0 dBW), which means that in the real case the communication blackout would not occur, as far as frequency synchronization is reached and the system parameters are correctly set.

In the **absence of plasma**, the attenuations are equal to 145 dB for the LHCP channel (i.e. LHC polarized receiving antenna) and 150 dB for the RHCP channel, including the atmosphere attenuation which is estimated equal to 0.075 dB (ITU model). In this case the receiver does not include the equalizer (not needed) and the losses are only due to the nonlinearity. Fig. 2 shows the channel bit error rates versus  $E_c/N_0$  where  $E_c$  is the received channel bit energy: the loss due to the nonlinearity is of about 0.3 dB; Fig. 3 shows on the left the channel BERs for the LHCP, RHCP channels and at the output of the combiner, and on the right the information BER and FER (1000 simulated frames) for the LHCP channel. The maximal ratio combiner actually allows to get a performance which is better than those of the single channels, but only when both the LHCP and RHCP channels provide channel BERs lower than 0.2. Note that, due to the different attenuations, the range of  $E_c/N_0$  in Fig. 2 is different for the LHCP and RHCP channels.

The transfer functions in the **presence of plasma** are shown in Fig. 4: dots represent the values provided by AIPT, while lines correspond to the interpolated channel transfer function simulated by DLBS. The power spectra of the signal at the output of the amplifier and of the signals received on the RHCP and LHCP channels are shown in Fig. 5: note the presence of sidelobes due to the nonlinearity of the amplifier and the presence of “holes” in the spectra of the received signals.

The attenuation at the center frequency  $f_c$  is equal to 171 dB for the LHCP channel and 167 dB for the RHCP channel, but the ratio between the transmitted and received power is equal to 184.9 dB for the LHCP and 181.9 dB for the RHCP channel. With respect to the ideal case, plasma reduces the received power by 39.9 dB and 31.9 dB on the LHCP and RHCP, respectively. The measured channel BER plots of Fig. 7 (on the left) allow to see that the loss due to plasma is actually smaller and amounts to 26 dB and 18 dB for the LHCP and RHCP, respectively, at BER=0.1. The presence of equalization at the receiver allows to reduce the loss due to intersymbol interference by 2-3 dB at channel BER values smaller than 0.01, but the gain due to the equalizer is much reduced if information BER and FER are considered (approximately 0.2 dB, as can be seen in plot on the right of Fig. 7).

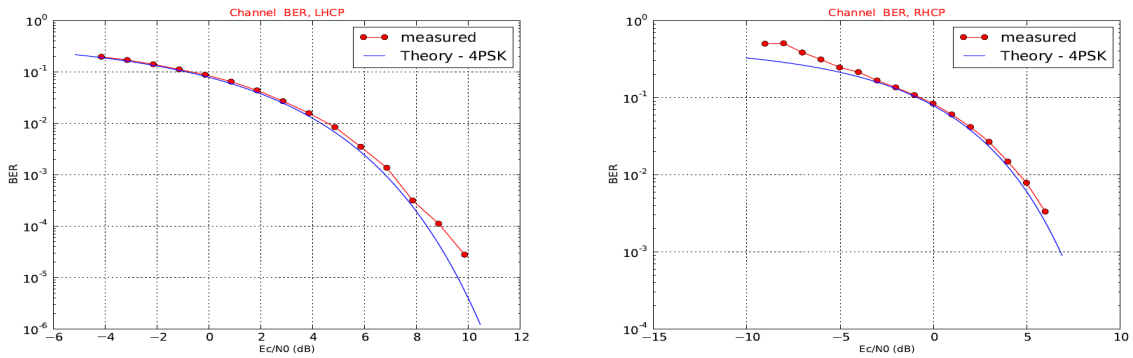


Fig. 2. Case of no plasma: channel BER vs.  $E_c/N_0$  for the LHCP and RHCP channels.

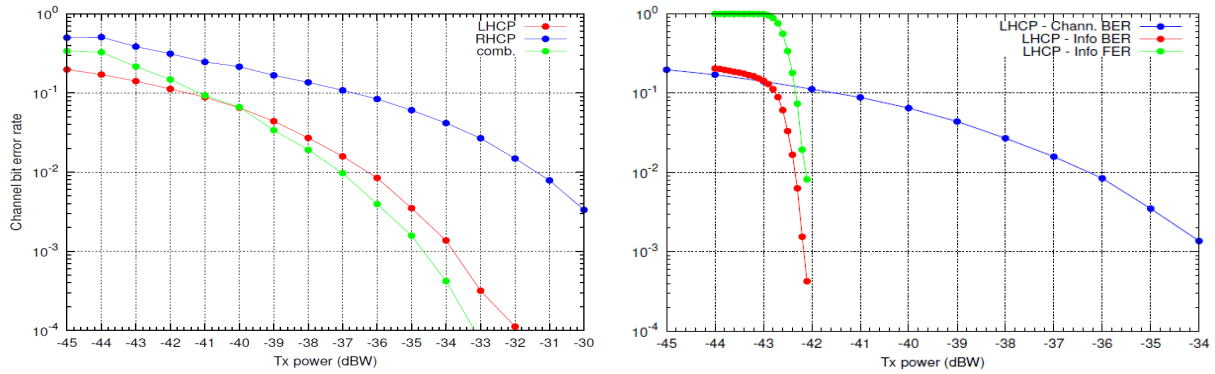


Fig. 3. Case of no plasma: channel BER for LHCP, RHCP and combined channels (left), information BER and FER compared to the channel BER for the LHCP channel (right)

B. Dynamic simulation

The telemetry link was again studied in dynamic conditions (average over the cone in terms of modulus and phase) for the case of transmitted power equal to -20 dBW. The number of simulated frames was 1000; since one frame interval is equal to 9.3 ms, the simulated time interval was equal to 9.3 s, which means that, according to (7), at the beginning the simulated transfer function was  $C(k\delta_f, 6\Delta_t)$  (corresponding to absolute time  $t=50$  s, Mach number 27, top of Fig. 7) and at the end it was practically  $C(k\delta_f, 7\Delta_t)$  (corresponding to absolute time  $t=60$  s, Mach number 25, bottom of Fig. 7). Fig. 8 shows the useful received power (measured for each of the 1000 frames) on the LHCP and RHCP channels, while Fig. 9 shows the evolution of channel BERs (number of errors in the bits of the  $k$ -th frame): the RHCP channel has a higher BER with respect to the LHCP channel, and the BER at the output of the combiner is always smaller than the other two BERs.

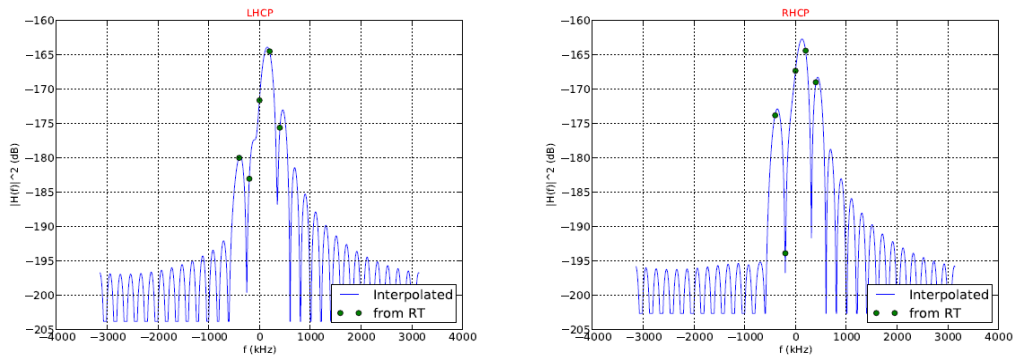


Fig. 4. Case of plasma: LHCP and RHCP channel transfer functions

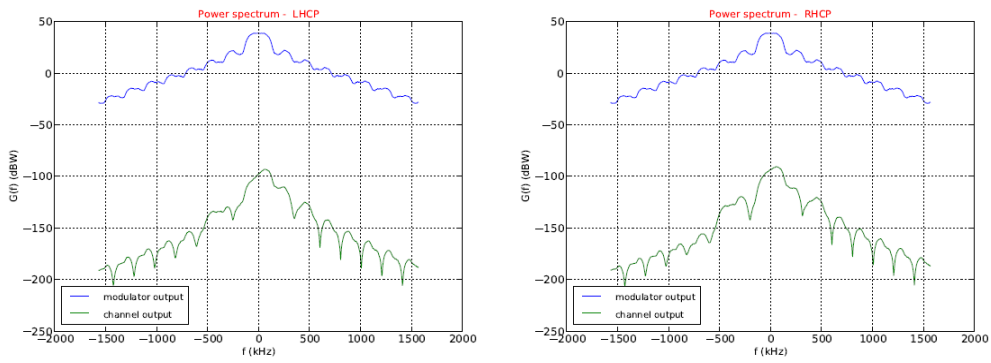


Fig. 5. Power spectrum of the signal at the output of the channel.

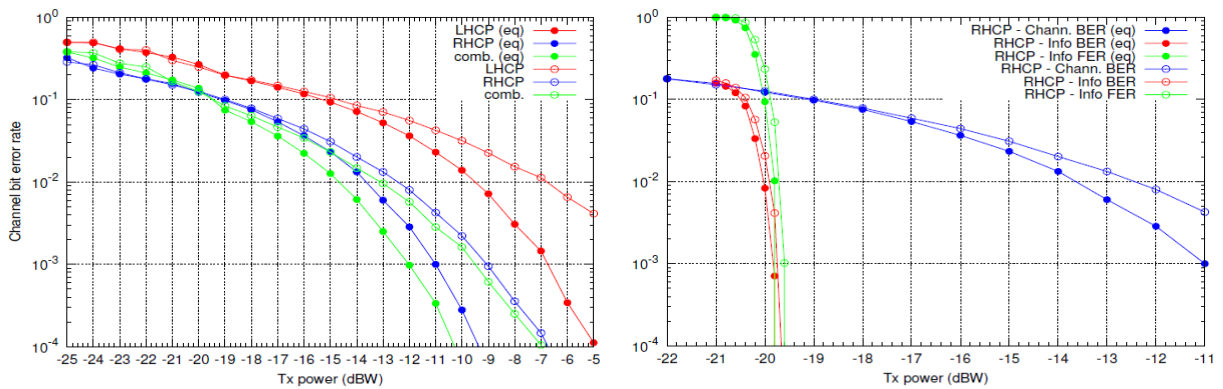


Fig. 6. Case of plasma: channel BER for LHCP, RHCP and combined channels (left), information BER and FER compared to the channel BER for the LHCP channel (right). The results are shown for the case of presence and absence of the equalizer.

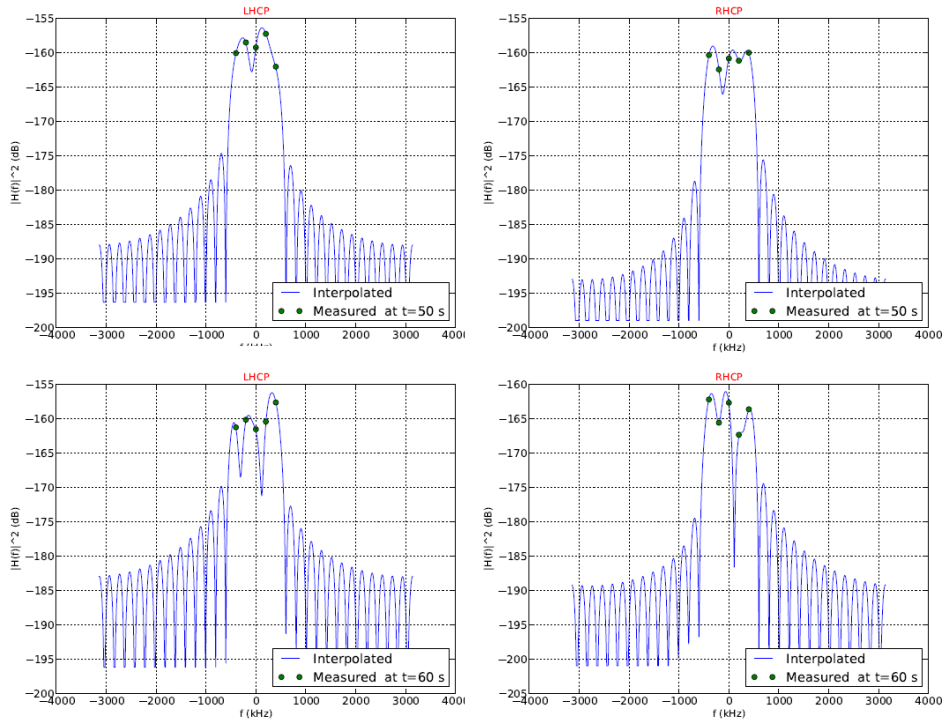


Fig. 7. Case of plasma: average channel transfer functions at  $t=50$  s and  $t=60$  s, for the dynamic simulation.

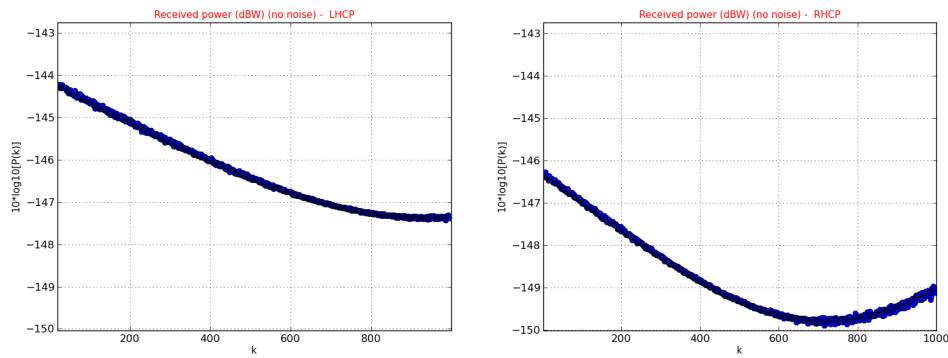


Fig. 8. Case of plasma, dynamic simulation: received useful power for each frame.

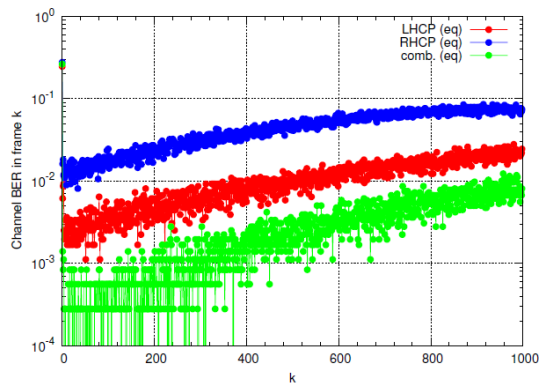


Fig. 9. Case of plasma, dynamic simulation: channel BER for each frame k.

## VI. CONCLUSIONS

The Dynamic Link Budget Simulator, together with AIPT, allows to study the dynamic performance of the time-varying link between a re-entry vehicle and a ground station. Thanks to this software, the user can optimize the link parameters: the position of the antenna onboard the vehicle, the modulation and coding schemes, the structure and parameters of the receiver etc. In the analyzed case the telemetry loss due to plasma amounts to 18 dB for the more favourable RHCP channel. In general both RHCP and LHCP channels should be used at the ground station, together with the signal processing techniques currently used in terrestrial wireless mobile communications, since the channel models have several similarities.

## REFERENCES

- [1] G. Vecchi, F. Vipiana, J. Tobon Vasquez, M. Visintin, F. Milani, M. Bandinelli, M. Sabbadini, *Reentry vehicles: evaluation of plasma effects on RF propagation*, TTC 2013
- [2] CCSDS Green Book 413.0-G-2, *Bandwidth-Efficient Modulations, Summary of Definition, Implementation and Performance*, October 2009
- [3] CCSDS Blue Book 414.1-B-1, *Pseudo-Noise (PN) Ranging Systems*, Issue 1, March 2009
- [4] W.L. Stutzman, G.A. Thiele, *Antenna theory and design*, Wiley, 1981
- [5] Rabiner Gold *Theory and Application of Digital Signal Processing*
- [6] S. Melloni, *Technical Report: REV-CT Project – Space to Ground Segment ICD (Interface Communication Document)*, RT/2011/147, May 2012
- [7] F. Milani, *Technical Report : ESA REV-CT Project– Final Report and Executive Summary*, RT/2012/025, May 2012
- [8] Python official website: <http://www.python.org/>